Surface defects and temperature on atomic friction

O Y Fajardo and J J Mazo

Departamento de Física de la Materia Condensada and Instituto de Ciencia de Materiales de Aragón, CSIC-Universidad de Zaragoza, 50009 Zaragoza, Spain

E-mail: yovany@unizar.es

Abstract. We present a theoretical study of the effect of surface defects on atomic friction in the stick-slip dynamical regime of a minimalistic model. We focus on how the presence of defects and temperature change the average properties of the system. We have identified two main mechanisms which modify the mean friction force of the system when defects are considered. As expected, defects change locally the potential profile and thus affect the friction force. But the presence of defects also changes the probability distribution function of the tip slip length and thus the mean friction force. We corroborated both effects for different values of temperature, external load, dragging velocity and damping. We show also a comparison of the effects of surface defects and surface disorder on the dynamics of the system.

(Some figures in this article are in colour only in the electronic version)

PACS numbers: 62.20.Qp, 81.40.Pq

Submitted to: *J. Phys.: Condens. Matter*

1. Introduction

Understanding friction is an actual scientific and technological problem [1, 2, 3]. Friction is a complex phenomenon of fundamental interest in many scientific areas that occur at all length scales [4, 5, 6, 7]. Its comprehension at the nanoscale is fundamental for instance for the manipulation of nanoparticles and the miniaturization of moving devices as nano-electromechanical systems (NEMs). With the development of experimental techniques such as the force friction microscope (FFM) and the surface force apparatus (SFA), experimental and theoretical studies of friction at the atomic scale have received an increasing interest in the last years. Furthermore, as the frictional interface between two surfaces involves complex interactions among many asperities, the atomic force microscope is an exceptional tool to better understand friction at nanoscale level since it can be described essentially as a single asperity dragged along a surface [4, 5, 8].

So far, most theoretical studies describing force friction microscopy (FFM) experiments have focused on the behavior of defect-free and perfect periodic surfaces with or without the inclusion of thermal effects [9, 10, 11, 12]. However, the study of the effect of substrate disorder or defects on atomic friction is particularly important since atomically flat surfaces represent ideal models and defects of different kind are always present. A recent study in a one-dimensional model indicates that small uncertainties in the interaction effective potential between the FFM tip and the surface can produce strong changes in the frictional behavior of the tip [13]. Other results shows that other kind of imperfections in the substrate potential also modify the frictional behavior at atomic scale [14, 15, 16]. Reguzzoni *et al* studied friction in the sliding of a xenon monolayer on a copper substrate [16]. They found that the onset of slip of the monolayer is strongly affected by the presence of vacancy-type defects within the monolayer. Hölscher et al analyzed the load dependence of atomic friction at atomic-scale surface steps [17].

In order to better characterize atomic-scale friction under realistic surface potentials we present here results for the effect of *surface defects* on atomic friction and its interplay with thermal effects. By surface defects we refer to absorbed molecules, vacancies or inclusion of attractive or repulsive atoms into the perfect lattice. We will use a minimalistic model which focuses in a small number of the most relevant degrees of freedom and emphasizes the nonlinear nature of frictional dynamics. We consider the one-dimensional case and focus on the stick-slip region of the friction force versus dragging velocity curve. The same problem has been studied previously by Tshiprut *et al* [14]. We present results for the mean value of the friction force and the slip length and for the slip length probability distribution functions (PDFs) for a range of values of the corrugation potential amplitude, density of defects, temperature, and damping. We present results for four different types of defects. Our results indicate that the presence of defects may strongly modify the frictional behavior at atomic scale. The observed changes in the friction force result from local changes of the potential profile, which in many cases produce also significant changes in the PDFs of the slip lengths. We

have compared our results with the defect-free case and evaluated how the inclusion of defects locally modify the slip length that the tip performs. To finish we make a detailed comparison of the results obtained for *surface disorder* and *surface defects*. We also observe that the effect of surface disorder on averaged quantities is screened at enough strong thermal fluctuations. On the contrary, for the surface defects problem we found significant effects even at high temperatures.

2. Model

We study a generalized Prandtl-Tomlinson model which includes the thermal effects[11],

$$\begin{aligned} M\frac{\mathrm{d}^2x}{\mathrm{d}t^2} + M\gamma\frac{\mathrm{d}x}{\mathrm{d}t} + \frac{\partial U(R,x)}{\partial x} &= \xi(t), \\ U(R,x) &= \frac{k}{2}\left[R(t)-x\right]^2 + V(x). \end{aligned} \tag{1}$$

Here the tip is modeled as a single particle dragged by an elastic spring over a one-dimensional substrate potential. $U(R,x)$ accounts for the tip effective potential and it includes the elastic coupling of the tip with a support which moves at constant velocity v_s ($R(t) = R_0 + v_s t$), and the tip-surface interaction $V(x)$. M and x are the effective mass and the lateral position of the tip and k is an effective spring constant. $\xi(t)$ is the random noise term which satisfies the fluctuation-dissipation relation $\langle\xi(t)\xi(t')\rangle = 2M\gamma k_{\mathrm{B}}T\delta(t-t')$ with γ the microscopic friction coefficient and k_{B} the Boltzmann constant.

We model surface defects by including gaussian terms in the standard tip-surface interaction potential,

$$V(x) = -U_0\left[1.0 + \cos\left(\frac{2\pi}{a}x\right)\right] + \sum_j A_0 \mathrm{e}^{-\frac{(x-x_j)^2}{2\sigma^2}}. \tag{2}$$

A_0 gives the amplitude of the defect potential and σ its range. a and U_0 are the lattice spacing and the amplitude of the defect-free surface potential, respectively. In theory, this amplitude can be changed by varying the normal load [12, 18].

We will show below results for the four kind of defects shown in figures 1(b)-(e). Panel (a) shows the potential profile for a perfect lattice. As in [14] we model the inclusion of atoms of different nature by introducing a random series of gaussian terms located in the minima ($x_j = na$) of the otherwise perfect lattice (see figure 1(b) where $A_0 = -0.71U_0$ and $\sigma = 0.2a$). The absence of atoms in the substrate is modeled introducing gaussian terms located randomly in the maxima [$x_j = (2n+1)a/2$] of the lattice (see figure 1(c) where $A_0 = -2.0U_0$ and $\sigma = 0.2a$). Figure 1(d) stands for defects located in the minima with $A_0 = +2.0U_0$ and $\sigma = 0.2a$; and figure 1(e) for defects in the maxima with $A_0 = +0.71U_0$ and $\sigma = 0.2a$. For the first two kinds of defects, figures 1(b)-(c), $A_0 < 0$ and we will refer to them as type I defects. For the last two cases, figures 1(d)-(e), $A_0 > 0$ and we will refer to them as type II defects.

To obtain dimensionless equations, energy can be measured in units of the corrugation potential amplitude U_0, space in units of the lattice spacing ($\widetilde{x} = 2\pi x/a$)

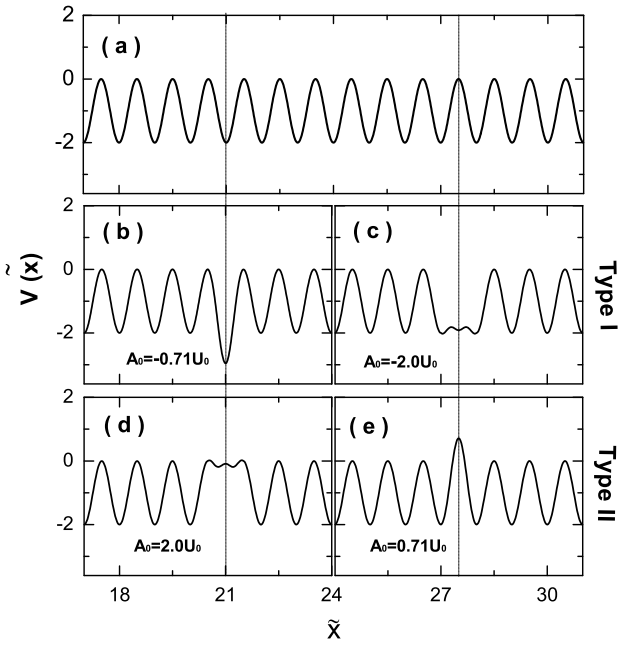

Figure 1. Tip-surface potential $V(\widetilde{x})/U_0$ for (a) the perfect lattice, (b) the type I defect-in-minima lattice, (c) the type I defect-in-maxima lattice, (d) the type II defect-in-minima lattice and (e) the type II defect-in-maxima lattice.

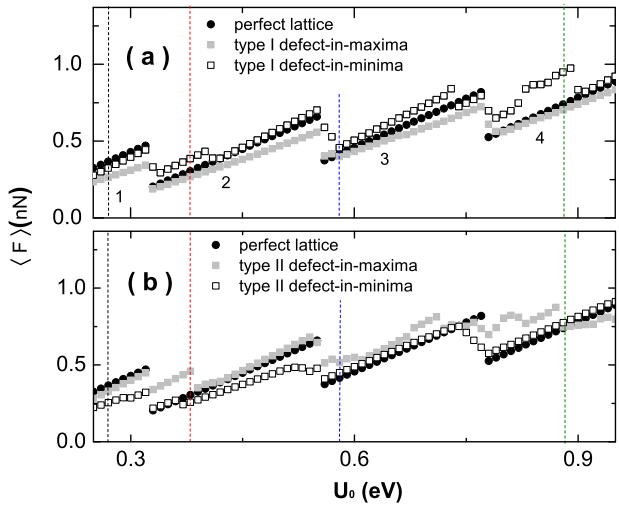

Figure 2. Average friction force versus corrugation potential amplitude U_0 in the low driving velocity region ($v_s = 10$ nm/s). $T = 0$ and $\gamma = 10^5 \mathrm{s}^{-1}$. (a) results for the defect-free (solid circles), type I defects-in-maxima (solid squares), and type I defects-in-minima (open squares)lattices. (b) results for the defect-free (solid circles), type II defects-in-maxima (open squares), and type II defects-in-minima (solid squares) lattices. The density of defects is $d = 30\%$.

and time in units of the natural frequency for oscillations of the tip in the surface

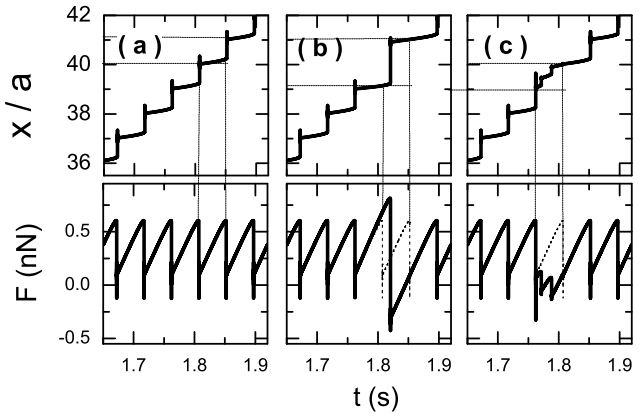

Figure 3. Figures (a) to (c) show the local effects of the inclusion of defects on the instantaneous position and friction force of the tip for $U_0 = 0.27$ eV. The density of defects is $d = 30\%$, $T = 0$ and $\gamma = 10^5 \mathrm{s}^{-1}$. (a) stands for the perfect lattice, (b) for type I in minima and (c) for type I in maxima.

potential ($\tau = \omega_p t$ with $\omega_p = 2\pi\sqrt{U_0/Ma^2}$). Then $\widetilde{\gamma} = \gamma/\omega_p$, $\widetilde{k} = 1/\Theta = ka^2/(4\pi^2 U_0)$ and $\widetilde{v_s} = v_s\sqrt{M/U_0}$ are the dimensionless damping, spring constant and velocity respectively. Some of our results will be shown as a function of U_0. From the above relations we see that a change in U_0 produces a change in both the dimensionless damping and velocity of the system.

We have performed detailed numerical simulations of the dynamics of the system at different parameter values. We will present results for the mean friction force $\langle F \rangle$, with $F(t) = k[R(t) - x(t)]$, mean slip length $\langle L \rangle$ and slip length PDFs. Following the work by Tshiprut et al [14], we have used $M = 5.0 \times 10^{-11}$Kg, $a = 0.45$nm, $k = 1.5$N/m, $\gamma = 10^5 \mathrm{s}^{-1}$ (except in section V where we change the damping) and U_0 in the 0.2eV to 1.2eV range (then $\widetilde{\gamma}$ goes from 0.3 to 0.1 and Θ from 4 to 25). For v_s we have used 10nm/s, [19]. Our simulations were performed using an stochastic Runge-Kutta method with dimensionless time step 0.01. Averages were computed after a sliding distance of 2000 lattice constants. An evolution of this length allows to obtain results of the average quantities with reliable statistics. We will show also the Probability Distribution Function of the slip lengths.

3. Surface defects without temperature

Here we consider the effect of surface defects in the deterministic dynamics of the system, $T = 0$ K. We focus on the stick-slip region of the force versus velocity characteristic curve. The well-known behavior of the friction force as a function of the potential amplitude for the defect-free lattice [4, 5, 8, 9, 10, 11, 12, 13, 14] is presented in figure 2 (solid circles). There, the friction force has been computed in the low driving velocity region ($v_s = 10$ nm/s) with U_0 ranging from 0.25 to 1.2

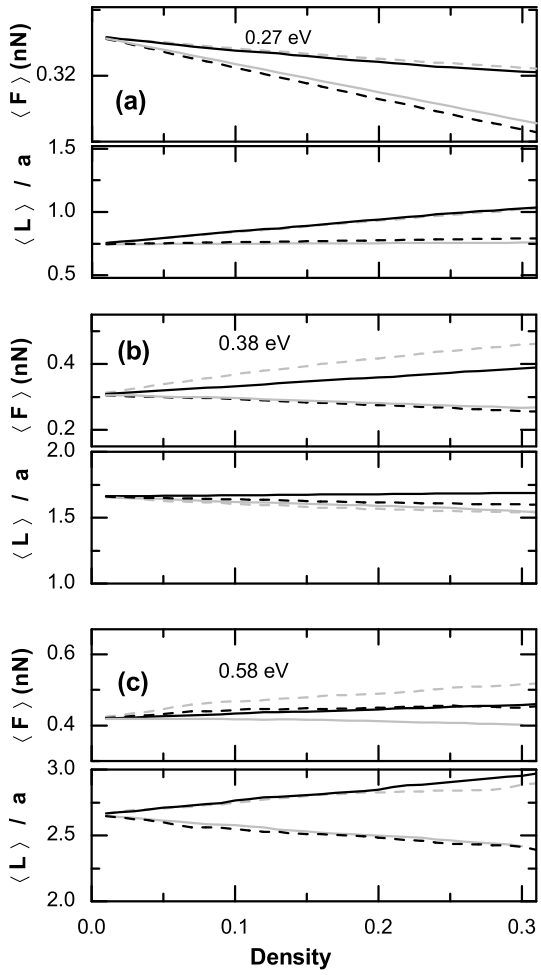

Figure 4. Average friction force and average length slip versus density of defects centered in minima (gray) or in maxima (black). Type I defects are continuous lines and type II dashed ones. We show results for $Uo = 0.27$ eV, $U_0 = 0.38$ eV, $U_0 = 0.58$ eV. $T = 0$ K and $v_s = 10$nm/s.

eV. A series of discontinuities can be seen. They mark transitions between different dynamical states characterized by a well defined mean value of the length of the slip events [9, 12, 13, 20]. Regions numbered as 1, 2, 3 and 4 in the figure correspond, respectively, to regions characterized approximately by one, two, three and four-lattice constant jumps. The value of the normalized parameter Θ in the first four regions is: $1.0 < \Theta_1 \leq 6.66 \leq \Theta_2 \leq 11.45 \leq \Theta_3 \leq 16.03 \leq \Theta_4 \leq 20.61$. For values of $\Theta < 1$, the tip slides smoothly and stick-slip events do not appear.

Figure 2 also presents the result for surface defects with density $d = 30\%$. As expected, in general the presence of type I defects in the potential minima or type II defects in the potential maxima increases the friction. On the contrary the suppression of potential maxima, type II defects in potential minima or type I defects in potential maxima, decreases friction. Thus, a system with both types of defects will suffer a certain balance of both effects. However, the dynamics of the system is much more complex

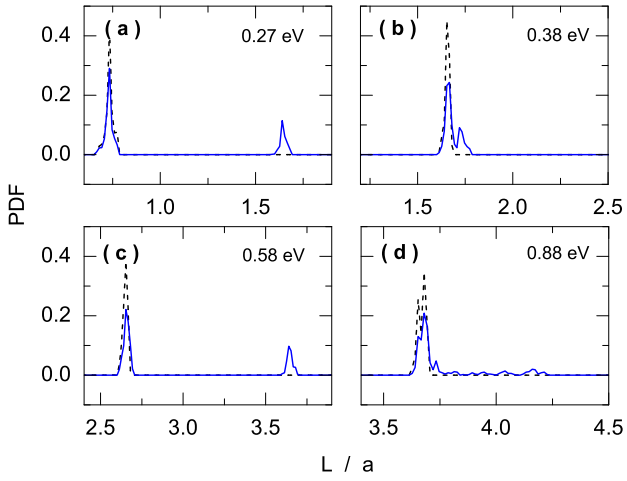

Figure 5. Probability density functions (PDF) of the slip length for the perfect (black dashed line) and the defect-in-minima (density 30%, solid blue line) lattices at $T = 0$ K and (a) $Uo = 0.27$ eV, (b) $U_0 = 0.38$ eV, (c) $U_0 = 0.58$ eV and (d) $U_0 = 0.88$ eV.

and this is not always the case. For type I in minima defects for instance, it is easy to see the presence of two competing effects: a deep potential causes a longer stick and then high friction, but it can also cause longer slips, which reduce friction. Depending on the parameter values the first or the second mechanism is the more important one. Furthermore, close to the transition points surface defect effects are difficult to predict. In addition, significant changes are observed for large values of the potential U_0. There, the effective damping is smaller [21] and the dynamics is more sensitive to small changes in the substrate potential.

Figures 3(a)-(c) show the effect of the surface defects on the instantaneous position of the tip (top) and friction force (bottom). Figure 3(a) stands for the perfect sinusoidal potential. This case is characterized by a regular tip dynamics with a characteristic slip length and a periodic friction force. The inclusion of type I defects in potential minima, figure 3(b), produces a significant change in the slip lengths and friction forces. Finally, type I defects in maxima, figure 3(c), produce a strong reduction of the slip length and a reduction of the stick phase. We have checked that as expected such reduction is complete if we totally remove the potential maximum.

Figures 2 and 3 were computed for a density of 30% of defects. In figure 4 we study the value of the mean friction force and mean slip length as a function of the density of defects (solid lines are for type I defects and dashed lines for type II ones) for three values of the potential amplitude: $U_0 = 0.27$, 0.38 and 0.58eV (marked in figure 2). We observe a significant modification of the friction force. As it can be seen in the figure, this change sometimes is associated to an important change of the mean slip length, and other times is due to the modification of the potential profile without change of $\langle L \rangle$. Figure also shows that the friction force and the slip length change linearly with the density of defects. Due to computational reasons, in what follows we will show results

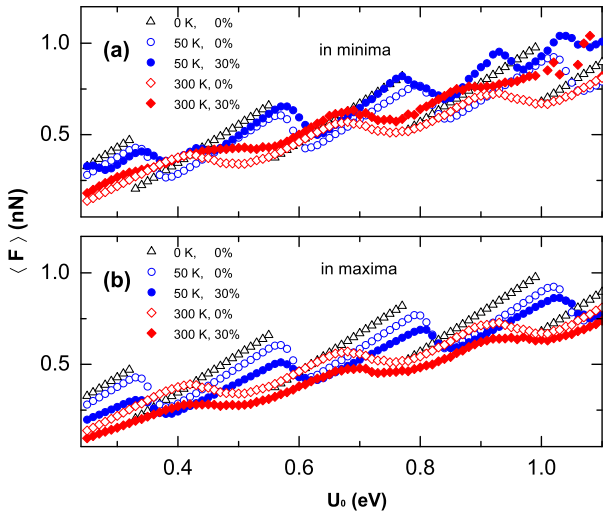

Figure 6. Average friction force versus corrugation potential amplitude U_0 at $T = 0$, 50 and 300 K. (a) Type I defect-in-minima and (b) type I defect-in-maxima case. Open symbols are the defect-free lattice and solid ones for surface defect ones. In all the cases $v_s = 10$nm/s.

for a density of defects $d = 30\%$.

In order to get a better insight of the findings showed in figure 4, we have computed slip length PDFs at different values of U_0, figure 5 for $d = 30\%$. We show results for the defect-free and type I defect-in-minima cases, other type of defects can be understood in a similar way. For $U_0 = 0.27$ eV [figure 4(a)], for the defect free case a single peak with $\langle L \rangle$ close to one is found [22] [black dashed line in figure 5(a)]. For the lattice with defects the slip length PDF (blue line) presents significant modifications. Now we see a second peak in the distribution, located near to $L/a = 1.65$ and a decrease of the original one located at $L/a = 0.73$. Thus the average slip length is increased and the friction force reduced. Larger densities produce an additional increase of the second peak and reduction of the first one.

For $U_0 = 0.38$ eV the mean slip length $L/a \simeq 1.65$ for all the defect density studied, figure 4(b). The corresponding PDF are also slightly modified as seen in figure 5(b). However, we observe an important increase of the friction force which in this case is ascribed to the increase in the potential barriers associated to the defects.

In the third case, $U_0 = 0.58$ eV, figure 4(c), we observe both effects: an important modification of the slip length PDF with an increase of the slip length mean value and also an increase of the friction force.

Finally, the last case shown in Figure 5(d), corresponds to a small normalized damping and there the dynamics of the tip is different. At low values of the normalized damping tip oscillations exist between the accessible wells. This effect introduces additional changes in the friction force and the slip length. These two combined effects, defects and low normalized damping, produce a slightly modified slip length but a

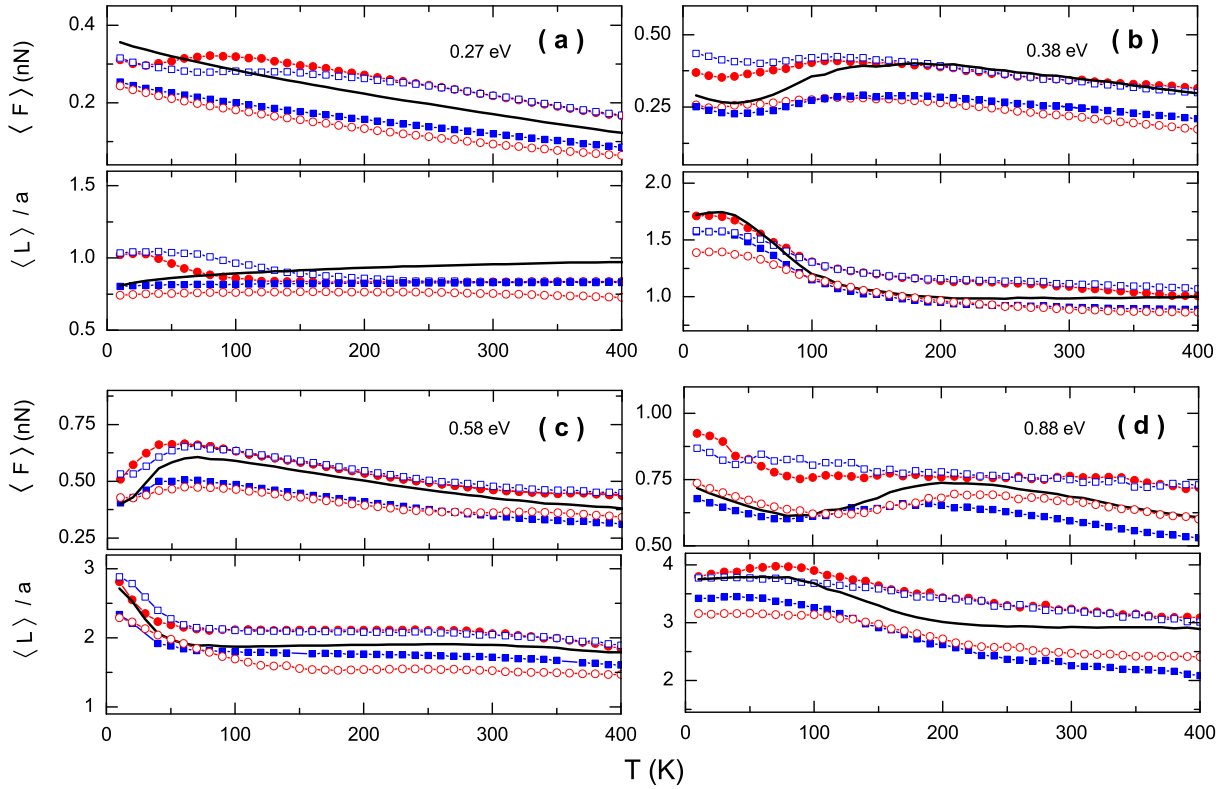

Figure 7. Average value of the friction force and the slip length versus temperature for different potential corrugation amplitudes U_0 for the defect-in-minima, defect-in-maxima and perfect (continuous black line) cases. Type I defect-in-minima (solid circles), type I defect-in-maxima (solid squares), type II defect-in-minima (open circles) and type II defect-in-maxima (open squares). U_0 =0.27, 0.38, 0.58 and 0.88 eV; panels (a) to (d) respectively. As usually $v_s = 10$nm/s.

significant change in friction force.

4. Surface defects with temperature

In this section we will present results on the combined effect of surface defects and temperature in the friction force of the system. Theoretical and experimental results have shown that thermal effects are fundamental to understand friction at this scale [10, 11, 14, 23, 24, 25, 13]. Previous studies show that the main temperature effect is a reduction of the friction force in the stick-slip region. This reduction, which has been observed at high temperatures, is explained in terms of thermally activated jumps of the tip [10, 11]. Recently, it has been also observed that, at low temperatures, thermal fluctuation can increase the friction force, which reaches a maximum and then decreases [13, 14, 24]. This effect is understood in terms of a reduction of the mean length of the slip events which dominates at low temperatures.

Due to the important role played by temperature it is natural to consider now

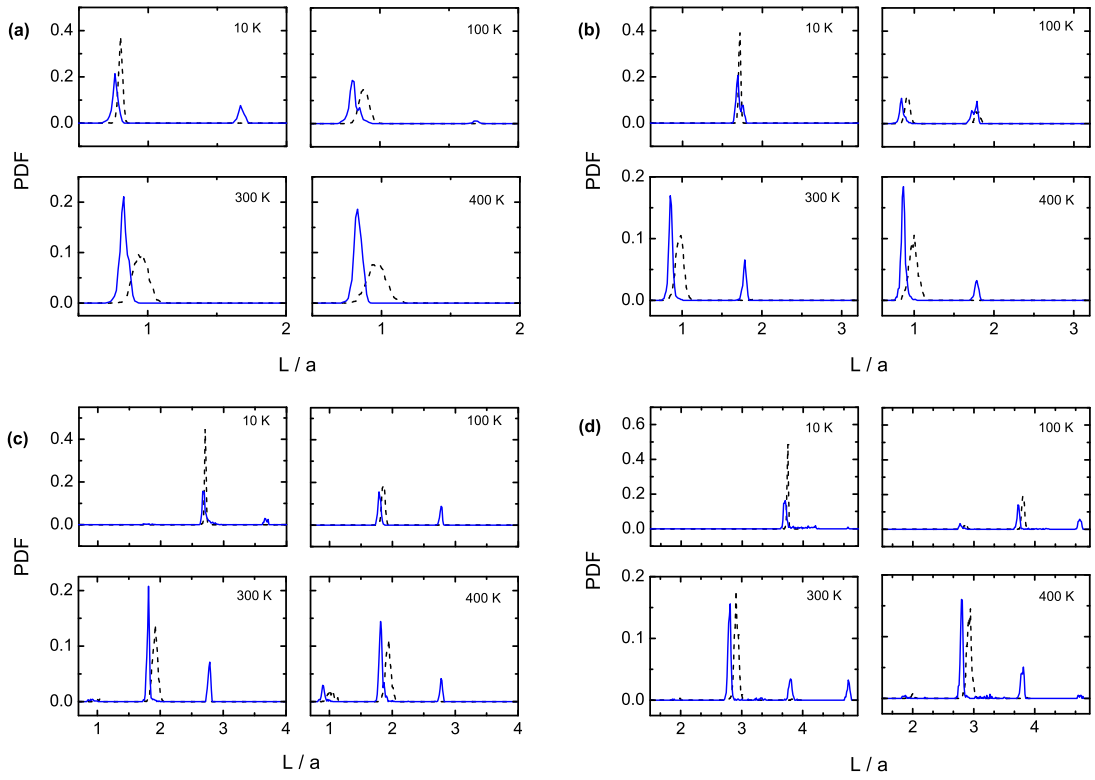

Figure 8. Slip length PDFs for the defect-free lattice (black dashed line) and the type I defect-in-minima one (blue line) at: (a) $U_0 = 0.27$, (b) $U_0 = 0.38$, (c) $U_0 = 0.58$, and (d) $U_0 = 0.88$ eV. For each potential value above we show the PDF at $T = 10$, 100, 300 and 400 K.

the combined effect of thermal fluctuations and surface defects in the response of the system. Figures 6, 7, 8, and 9 summarize the main results. In figure 6(a) we compare at $T = 0$, 50 and 300 K, the average friction force versus the potential amplitude U_0 for the defect-free lattice (open symbols) and the type I defect-in-minima. In figure 6(b) we show the same comparison for the type I defect-in-maxima case. Differences are clearly visible in all the studied temperature range. This effect is also studied in figure 7 where we show the average friction force $\langle F \rangle$ and slip length $\langle L \rangle$ as a function of the system temperature for four different values of U_0 corresponding to the four different dynamical states marked in figure 2.

The inclusion of surface defects does not modify the two main competing thermal effects already reported in the literature. The low U_0 and high temperature regimens are dominated by a monotonic decreasing of friction due to thermal activation without modification of the mean slip length. At low temperatures and high U_0 values, friction increases due to the reduction of the mean slip length [13]. However we observe that at a given temperature the friction force for the type I defect-in-minima case is bigger than for the defect-free one which in turns is also bigger than for the type I defect-in-maxima lattice.

In figure 8 we show the change in the probability distribution functions by the

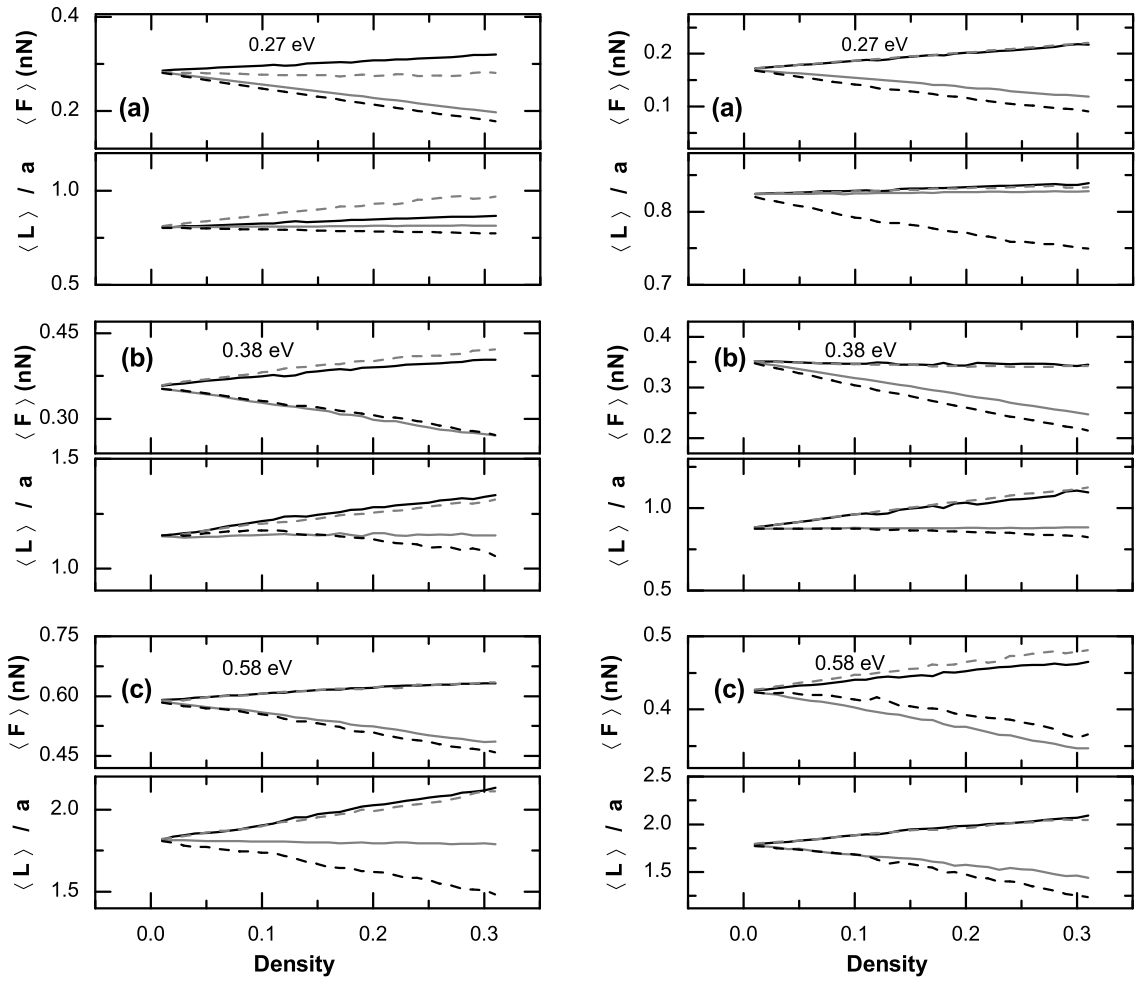

Figure 9. Average friction force and average length slip versus density of defects centered in minima (gray) or in maxima (black) . Type I defects are continuous lines and type II dashed ones. We show results for $Uo = 0.27$ eV, $U_0 = 0.38$ eV, $U_0 = 0.58$ eV at $v_s = 10$nm/s and $T = 100$K (left) and 300K (right).

combined effect of defects and temperature. We present results for type I defect-in-minima. The figure shows the results for the same U_0 values used in figure 5 but now at four different temperature values. In the first case ($U_0 = 0.27$ eV), figure 8(a), temperature suppress the second peak of the PDF. In this case temperature affects more importantly the defect-free case and moves apart the location of the peaks. For $U_0 = 0.38$ eV, figure 8(b), temperature activates a second peak close to $\langle L \rangle = 1$. As temperature increases the original one decreases and disappears for the defect-free lattice case. For $U_0 = 0.58$ eV, figure 8(c), at zero temperature the main peak is observed close to $\langle L \rangle = 3$. At higher temperatures we observe first the appearance of a second peak close to $\langle L \rangle = 2$, which will become the more important one, and later a third one close to $\langle L \rangle = 1$. At $U_0 = 0.88$ eV, figure 8(d), the normalized damping is smaller and dynamics is more complex and oscillations between adjacent wells are possible.

An important consequence of figures 7 and 8 is that although the PDF for the

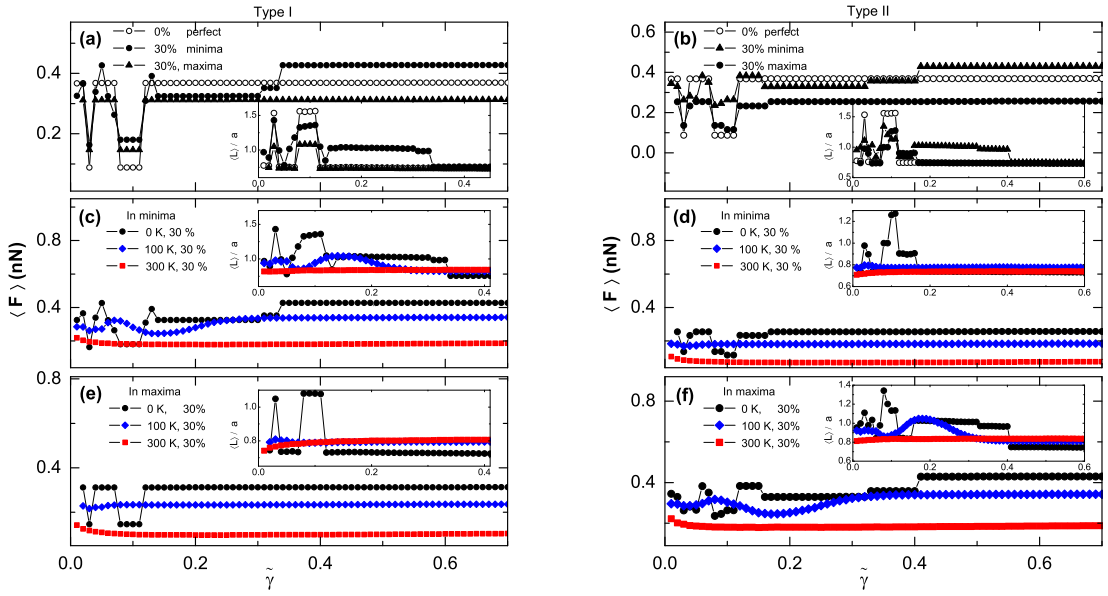

Figure 10. The mean friction force and mean slip length versus normalized damping at $T = 0$ K for perfect lattice (open symbols), defects in minima of lattice and defects in maxima of lattice. (a) Type I defects and (b) type II defects. Combined effect of surface defects and temperature (circles for $T = 0$, diamonds for 100 and squares for 300 K) on the mean friction force and mean slip length as a function of normalized damping for defects in minima and defects in maxima of lattice. (c),(e) for type I and (d),(f) for type II defects. In all cases $U_0 = 0.27$ eV and 30 % for density of defects.

lattice with and without defects can be quite similar (especially at low T) the mean friction force is very different due to reduction of the effective barrier of the system.

Finally, we have studied again the dependence of the friction force and mean slip length as a function of the density of defects in the surface. In figure 4 we showed the results for the zero temperature case. Now, in figure 9 we plot the similar results for $T = 100$K and $T = 300$K. As we can see in the figures at all the temperatures, both, the mean friction force and the mean slip length depend almost linearly on the density of defects for the studied range

5. Damping effect

The effect of coupling of the system to many other degrees of freedom is modeled by assuming the existence of a heat bath at a given temperature and satisfying the fluctuation-dissipation relation. The dissipation associated with this coupling is controlled by the damping parameter, with temperature being a well-controlled parameter. However to determine the correct value of the effective damping for the tip is a much more complex and difficult question. Thus, it is important to study the dynamics of the system for different values of the damping in order to check the robustness of the results against changes of this important parameter of the dynamics of the system.

A critical damping value is usually defined above which the tip oscillations disappear (overdamped dynamics). In this case all the deterministic slips have a length close to one lattice constant. However, there are experimental evidences which indicate that the damping of the system is below this critical value. In this case the dynamics is more complex and richer [26, 27]. We have studied first in the regular case the effect of the damping parameter on the friction force for values of $\widetilde{\gamma}$ crossing the critical value. Then we analyze how this behavior is affected when surface defects are included. In figure 10(a) we observe a series of steps in the friction force versus damping curve (open symbols). Close to the discontinuities a small change in the damping can produce a large change in the friction force. Every step in figure corresponds to a slip close to one or two lattice sites respectively. In the overdamped limit only the first available minimum (site 1) is reached. When smaller values of the damping are achieved the tip can reach a further minimum (site 2). If damping is reduced again the tip can move through 1 to 2 and then oscillates back to 1 where is trapped. At small damping the tip oscillates back and forth between both minima before reaching an equilibrium value. Then, by decreasing the value of the damping more transitions are observed. For other values of the parameters (larger U_0), more complex situations are found. In these cases dynamics results from the interplay between a larger number of minima than that shown in figure 10.

When surface defects are included (full symbols), additional slight modifications are observed. Figure 10(a) shows the change of the friction force and the mean slip length as a function of the damping for a density of 30% of defects and it compares to the regular case curve. With inclusion of the thermal effects (diamond symbols, 100 K), the steps are strongly smoothed, see figure 10(b). At higher temperatures steps are strongly smoothed or even suppressed (square symbols, 300 K).

6. Discussion and conclusions

We have studied the effect of the presence of four different types of surface defects on atomic friction. Our results show that significant changes can be observed even at high temperature. As expected, differences are more important for U_0 values close to deterministic dynamical transition points of the system.

As we have seen, for surface defects, the change in the mean friction force can not be understood in terms of the change in the mean slip length. In order to understand our numerical results we have done an study of the probability distribution function of the slip length. A rich scenario where jumps of very different length may coexist is found.

We have identified two main different mechanisms which modify the mean friction force of the system when defects are considered. First, defects modify locally the potential profile in a way that change importantly the instantaneous friction force that the tip experiences when crosses one defect. Second, the presence of defect also changes the slip length probability distribution which also changes the mean friction force.

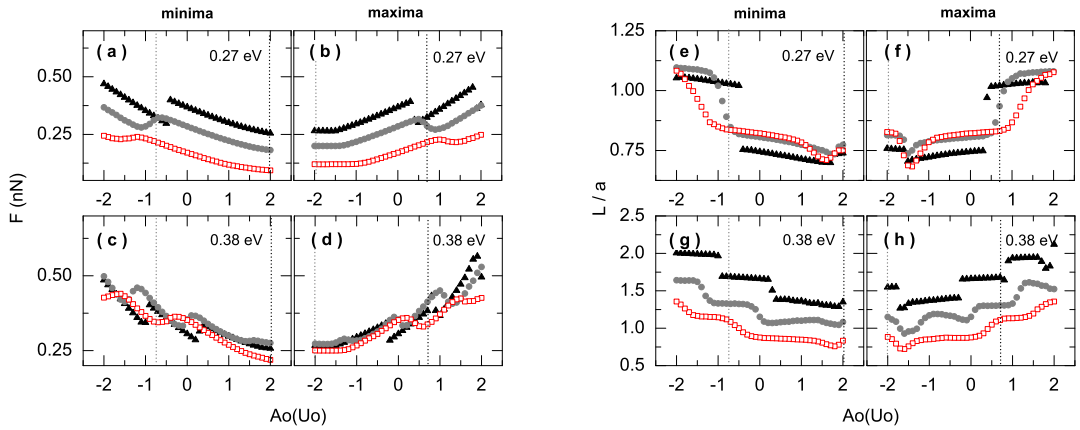

Figure 11. Friction force and mean slip length dependence on the amplitude of the defect potential A_0 for defects in minima and in maxima at $T = 0$ (black triangles), 100 (gray circles) and 300K (red squares)

With respect to the density of defects in the system, our results show an almost linear dependence on this parameter. We will discuss now on a different point which is related with the amplitude of the defect potential given by A_0. We have chosen $A_0 = -0.71U_0$ for type I defect in minima and $A_0 = 0.71U_0$ for type II defect in maxima and $A_0 = -2U_0$ for type I defect in maxima and $A_0 = 2U_0$ for type II defect in minima. Those values were chosen to get the potential profiles showed in figure 1. However other values of A_0 can be of interest for a particular real situation. Figure 11 shows the results of the mean friction force and mean slip length dependence on the defect amplitude coefficient A_0. Type I defects correspond to $A_0 < 0$ values and type II to $A_0 > 0$ values. Results are given for three temperature values (0, 100 and 300K) and two U_0 values (0.21eV and 0.38ev), showing two different physical situations. The figure shows that the friction force also depends importantly on this parameter in a way that is comparable to the effect of temperature or density defects. Figure also shows that, as expected, results for defect in minima and in maxima with different sign of A_0 are very similar. This was also shown in figures 4, 7 and 9 for instance.

To finish, we find interesting to compare our results for surface defects to the recently studied effect of surface disorder [13]. There, surface disorder was modeled including a small second harmonic term in the standard tip-surface interaction potential,

$$V(x) = -U_o \left[1.0 + \epsilon \ \sin\left(\frac{2\pi x}{b}\right)\right] \cos\left(\frac{2\pi x}{a}\right). \tag{3}$$

Thus the surface disorder changes the potential profile, introduces a distribution of barrier heights and moves slightly the positions of the potential maxima and minima.

Figure 12 compares the results obtained for the case of the perfect lattice, surface disorder and surface defects. It shows the results for $T = 0$K y $T = 300$K and at different values of U_0. The figure shows results for type I defects in minima and maxima. Similar results for other types of defects are found. At low temperature we found that it is not easy to distinguish between the presence of defects and disorder. However, an analysis

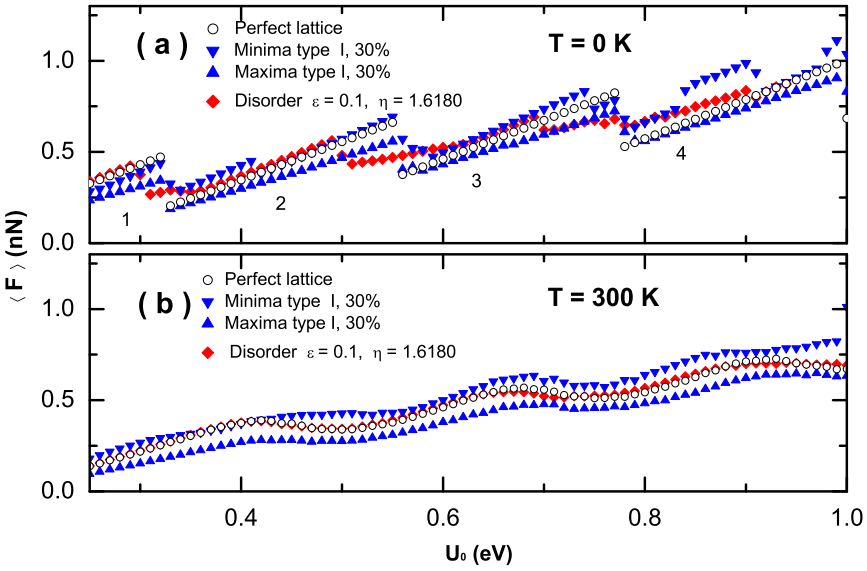

Figure 12. (a) Mean friction force versus corrugation potential amplitude U_0 at $T = 0$ K. We compare the effects from two representative types of surface defects on the friction force-corrugation potential curve of the perfect lattice (open circles): type I surface defects in maxima (solid triangles up), in minima (solid triangles down) and the effect of surface disorder (solid diamonds). In (b) the similar comparison at $T = 300$ K.

of instantaneous quantities such as force and tip position allows to discriminate both situations. At high enough temperature our results indicate that the role of the surface disorder is screened by the thermal effects but the presence of surface defects modifies the friction force of the system. In the regular and in the lattice with disorder the mean value of the barrier that the tip experiences is the same. However the presence of surface defects increases or decreases, depending on the type of the defects, the value of such mean barrier.

Our model accounts for the effect of adsorbed molecules or vacancies in the lattice, but it could be used also to study artificially designed grooves or ridges. Our results show that a significant density of defects in a sample may change the friction force curve at any temperature and thus such presence affects a comparison between numerical and experimental results.

However, it is important to point that friction is a very general phenomenon which occurs in several problems. Because of that, the study of simple models is important since it allows for understanding basic effects that can be relevant or realized in different kind of systems. This is the case for instance of the motion of a single colloidal particle in a colloidal system. There are now experiments and simulations where a single colloidal particle can be driven through other particles or quenched disorder and the effective friction and drag measured for varied temperature, density, pull rate and so forth [28, 29, 30, 31]. Some similar variations on the system can be rapidly realized by driving a single particle over a random, periodic or combination of periodic and random

substrates in 1D, 2D and even 3D so that some of the results from the present work could be tested more directly on real systems.

Another system where the results of the present paper could be applied is that of vortices in type-II superconductors. Very recent experiments drag individual vortices over random or periodic pinning arrays [32, 33, 34]. It would be interesting to make a periodic 1D or 2D pinning potential and drag a single vortex. This experiment could then be repeated for adding additional defects that could act like attractive or repulsive sites.

Acknowledgments

The authors acknowledge financial support from Spanish MICINN through project No. FIS2008-01240, cofinanced by FEDER funds. O. Y. Fajardo acknowledges financial support from FPU grant by Spanish MICINN.

References

[1] Bowden F P and Tabor D 1954 *The friction and lubrication of solids* (Oxford: Oxford University Press)
[2] Singer I L and Pollock H M 1992 *Fundamentals of frictions: macroscopic and microscopic processes* (Dordrecht: Kluwer Academic Publishers)
[3] Persson B N J and Tosatti E 1996 *The friction and lubrication of solids* (Dordrecht: Kluwer Academic Publishers)
[4] Gnecco E and Meyer E 2007 *Fundamentals of friction and wear on the nanoscale* (Berlin: Springer)
[5] Urbakh M, Klafter J, Gourdon D, and Israelachvili J 2004 *Nature* **430** 525
[6] Bormuth V, Varga V, Howard J, and Schäffter E 2009 *Science* **325** 870
[7] Urbakh M and Meyer E 2010 *Nature Materials* **9** 8
[8] Szlufarska I, Chandross M, and Carpick R W 2008 *J. Phys. D.:Appl. Phys.* **41** 123001
[9] Johnson K L and Woodhouse J 1998 *Tribol. Lett.* **5** 155
[10] Gnecco E, Bennewitz R, Gyalog T, Loppacher Ch, Bammerlin M, Meyer E, and Güntherodt H J 2000 *Phys. Rev. Lett.* **84** 1172
[11] Sang Y, Dube M, and Grant M 2001 *Phys. Rev Lett.* **87** 174301–1
[12] Medyanik S N, Liu W K, Sung I, and Carpick R W 2006 *Phys. Rev. Lett.* **97** 136106
[13] Fajardo O Y and Mazo J J 2010 *Phys. Rev. B* **82** 035435
[14] Tshiprut Z, Zelner S, and Urbakh M 2009 *Phys. Rev. Lett.* **102** 136102
[15] Braiman Y, Hentschel H G E, Family F, Mark C, and Krim J 1999 *Phys. Rev. E* **59** R4737
[16] Reguzzoni M, Ferrario M, Zapperi S, and Righi M C 2009 *Proc Natl Acad Sci USA* **107** 1311
[17] Hölscher H, Ebeling D, and Schwarz U D 2008 *Phys. Rev. Lett.* **101** 246105
[18] Socoliuc A, Bennewitz R, Gnecco E, and Meyer E 2004 *Phys. Rev. Lett.* **92** 134301
[19] Sang et al [11] used $a = 0.4$nm, $k = 0.93$N/m, $U_o = 0.27$eV, $\gamma = 8.9 \times 10^5 \mathrm{s}^{-1}$, $M = 8.7 \times 10^{-12}$kg, and $v_s = 25$nm/s which corresponds to $\widetilde{\gamma} = 0.804$ and $\Theta = 11.48$
[20] Nakamura J, Wakunami S, and Natori A 2005 *Phys. Rev. B* **72** 235415
[21] A change in U_o also changes the effective damping of the system since $\widetilde{\gamma} = \gamma/\omega_p$ and $\omega_p = 2\pi\sqrt{U_0/Ma^2}$. Thus a high load implies a smaller effective damping and it allows longer slip events
[22] We want to mention that due to the existence of an early creep stage in the movement of the tip before each slip event, the slip length is not exactly equal to a multiple of the lattice constant

[23] Sills S and Overney R M 2003 *Phys. Rev. Lett.* **91** 095501
[24] Schirmeisen A, Jansen L, Holscher H, and Fuchs H 2006 *Appl. Phys. Lett.* **88** 123108
[25] Riedo E and Gnecco E 2004 *Nanotechnology* **15** S288
[26] Kerssemakers J and Hosson J Th M 1995 *Appl. Phys. Lett.* **67** 347
[27] Roth R, Glatzel G, Steiner P, Gnecco E, Baratoff A, and Meyer E 2010 *Tribol. Lett.* **39** 63
[28] Habdas P, Schaar D, Levitt A C, and Weeks E R, 2004 *Europhys. Lett.* **67** 477
[29] Reichhardt C and Reichhardt C J O 2004 *Phys. Rev. Lett.* **92** 108301
[30] Reichhardt C J O and Reichhardt C 2008 *Phys. Rev. E* **78** 011402
[31] Mejia-Monasterio C and Oshanin G 2011 *Soft Matter* **7** 993
[32] Straver E W J, Hoffman J E, Auslaender O M, Rugar D and Moler K A 2008 *Appl. Phys. Lett.* **93** 172514
[33] Auslaender O M et al 2009 *Nature Phys.* **5** 35
[34] Reichhardt C 2009 *Nature Phys.* **5** 15